Available online at www.sciencedirect.com
ScienceDirect
Biochemical and Biophysical Research Communications 351 (2006) 44–50
BBRC
www.elsevier.com/locate/ybbrc

Characterization of the *Rana grylio* virus 3β-hydroxysteroid dehydrogenase and its novel role in suppressing virus-induced cytopathic effect

Wei Sun, Youhua Huang, Zhe Zhao, Jianfang Gui, Qiya Zhang *

State Key Laboratory of Freshwater Ecology and Biotechnology, Institute of Hydrobiology, Chinese Academy of Sciences, Graduate University of Chinese Academy of Sciences, Wuhan 430072, China

Received 26 September 2006
Available online 23 October 2006

Abstract

The 3β-hydroxysteroid dehydrogenase (3β-HSD) isoenzymes play a key role in cellular steroid hormone synthesis. Here, a 3β-HSD gene homolog was cloned from *Rana grylio* virus (RGV), a member of family *Iridoviridae*. RGV 3β-HSD gene has 1068 bp, encoding a 355 aa predicted protein. Transcription analyses showed that RGV 3β-HSD gene was transcribed immediate-early during infection from an initiation site 19 nucleotides upstream of the translation start site. Confocal microscopy revealed that the 3β-HSD-EGFP fusion protein was exclusively colocalized with the mitochondria marker (pDsRed2-Mito) in EPC cells. Upon morphological observation and MTT assay, it was revealed that overexpression of RGV 3β-HSD in EPC cells could apparently suppress RGV-induced cytopathic effect (CPE). The present studies indicate that the RGV immediate-early 3β-HSD gene encodes a mitochondria-localized protein, which has a novel role in suppressing virus-induced CPE. All these suggest that RGV 3β-HSD might be a protein involved in host-virus interaction.

Keywords: Iridovirus; *Rana grylio* virus (RGV); 3β-Hydroxysteroid dehydrogenase (3β-HSD); Immediate-early gene; Subcellular localization; Mitochondria; Cytopathic effect (CPE)

Rana grylio virus (RGV) is a pathogenic agent that has resulted in high mortality in cultured pig frog (*R. grylio*) [1]. It has been revealed that RGV is a large DNA virus similar to frog virus 3 (FV3) [2,3], the type species of genus *Ranavirus* (family *Iridoviridae*) [4]. The iridovirus genes are expressed in three main temporal kinetic expression classes: immediate-early (IE), delayed-early (DE) or early (E), and late (L), which can be defined experimentally by using protein synthesis and DNA replication inhibitors [5,6]. Generally, the products of viral IE genes are often transcription factors or other proteins involved in host-virus interaction [5–7].

The 3β-hydroxysteroid dehydrogenase/Δ^5–Δ^4isomerase (3β-HSD) enzyme catalyzes the conversion of Δ^5-3β-hydroxysteroids to Δ^4-3-ketosteroids, and thus plays an essential role in the biosynthesis of all classes of steroid hormones. Multiple isoforms of 3β-HSD have been identified in human, mouse, and rat [8], and its homologs have also been revealed in viruses [9–11]. The vertebrate 3β-HSDs were verified to have dual localization with the endoplasmic reticulum (ER) and mitochondria [8], whereas the intracellular localization of virus-encoded 3β-HSD (v3β-HSD) still remains unclear. Previous studies of v3β-HSD were mainly focused on mammalian virus, such as vaccinia virus [9,10,12]. The studies showed that the vaccinia virus 3β-HSD could suppress the inflammatory response to infection and thus contribute to virulence [9]. However, in iridoviruses, no further work has been done on the research of v3β-HSD except for some computer analyses [13,14]. In this study, we cloned a 3β-HSD gene from RGV, for the first time identified its characterization of

* Corresponding author. Fax: +86 27 68780123.
E-mail address: zhangqy@ihb.ac.cn (Q. Zhang).

0006-291X/$ - see front matter © 2006 Elsevier Inc. All rights reserved.
doi:10.1016/j.bbrc.2006.09.169

transcription and subcellular localization, and further did a preliminary investigation on its role during virus infection *in vitro*.

Materials and methods

Virus and cell. Propagation of RGV and isolation of the virus genomic DNA were performed as described previously [3]. *Epithelioma papulosum cyprini* (EPC) cell was maintained in TC199 medium supplemented with 10% fetal bovine serum (FBS) at 25 °C.

Gene cloning, plasmid construction, and computer-assisted analysis. The complete 3β-HSD gene was cloned by PCR from RGV genomic DNA using a pair of primers, P1/P2 (P1, 5′-TCTGAAACATCCCAAACAC-3′; P2, 5′-CCCGTAAAGAATCTATACCC-3′), which were designed according to the conserved flanking sequences of the putative v3β-HSD gene in FV3 and tiger frog virus (TFV) genomes [13,14]. The produced fragment was then cloned into pMD 18-T vector (TaKaRa) and sequenced. Two pairs of primers, P3/P4 (P3, 5′-TCAGAAGCTTGATA GAGATGGTAAAAT-3′, *Hin*dIII; P4, 5′-TCATTGGATCCCTTCA GAGTGCTTAT-3′, *Bam*HI) and P5/P6 (P5, 5′-GGATCCACG AGATGGTAAAATA-3′, *Bam*HI); P6, 5′-CTCGAGTTACTTCAG AGTGCTTAT-3′, *Xho*I, were used for plasmid construction. 3β-HSD gene fragments, amplified by paired primers P3/P4 and P5/P6, were subcloned into eukaryotic expression vectors pEGFP-N3 (Clontech) and pcDNA3.1 (Invitrogen), respectively, to obtain plasmids pEGFP-HSD and pcDNA3.1-HSD. The constructs were confirmed by restriction enzyme digestion and nucleotide sequence analysis. Database similarity searches were carried out by using the BLAST server [15]. Alignment of amino acid sequences was carried out using ClustalX 1.83 [16] and edited by GeneDoc program.

Rapid amplification of 5′ cDNA end (5′-RACE). The 5′ cDNA end of RGV 3β-HSD gene was determined by using 5′-full RACE core set (TaKaRa). Briefly, total RNA was extracted from RGV-infected EPC cells at a multiplicity of infection (MOI) of 1 at 12 h post-infection (p.i.) using TRIzol reagent (Invitrogen). The first strand cDNA was obtained by reverse transcription with a 5′-phosphated primer RACE-RT (5′-(p)TGCTCAGGGGGTAG-3′) and 5 μg of the obtained total RNA at 50 °C for 1 h, and then the product was degraded by RNase H for 1 h at 37 °C. The released cDNA was ligated to circular cDNA with T4 RNA ligase for 18 h at 16 °C. Thereafter, two rounds of PCR amplifications were carried out by using the first round primers S1/A1 (S1, 5′-GT GGTACAGACACACTGATGA-3′; A1, 5′-GATGTGAGAGATGTT TATGTCG-3′) and the second round of nest-PCR primers S2/A2 (S2, 5′-ACCTCTGGAGTGTTTGTGA-3′; A2, 5′-ATGTGACTGCCCAA GAATC-3′). The nest-PCR products were cloned into pMD 18-T vector (TaKaRa) and sequenced.

Temporal transcription analysis and drug inhibition assay. EPC monolayer cells were infected or mock-infected with RGV at an MOI of 1 and harvested at 0, 4, 8, 12, 16, 24, 36, and 48 h p.i. Total RNA was extracted from the harvested samples with TRIzol reagent (Invitrogen) and digested with RNase-free DNase I (TaKaRa) before carrying out the RT-PCR and direct PCR amplification. A pair of RGV 3β-HSD gene-specific primers, P7/P8 (P7, 5′-AGTTTTTCCACGACACGG-3′; P8, 5′-GAATGGGA GACCTCTTTACT-3′), was used to perform RT-PCR and PCR. Detection of *β-actin* mRNA was taken as an internal control by RT-PCR using paired primers Actin-F/Actin-R (Actin-F, 5′-CACTGTGCCCATCTAC GAG-3′; Actin-R 5′-CCATCTCCTGCTCGAAGTC-3′).

Cycloheximide (CHX), as de novo protein synthesis inhibitor, and cytosine arabinoside (AraC), as DNA replication inhibitor, were utilized to classify the transcript of RGV 3β-HSD gene. Briefly, EPC monolayer cells were pretreated with 50 μg/ml CHX or 100 μg/ml AraC for 1 h prior to and throughout the viral infection. CHX-pretreated cells were infected or mock-infected with RGV at an MOI of 1 and harvested at 6 h p.i., Simultaneously, AraC-pretreated EPC cells were infected or mock-infected with RGV at an MOI of 1 and harvested at 48 h p.i. RNA isolation and RT-PCR analysis for 3β-HSD gene were performed as described above. For control, two pairs of primers, DUT-F/DUT-R (DUT-F, 5′-TGGTCCCCTCCTTTGGCAG-3′; DUT-R, 5′-ACCCCTGTCGGT AGAGTCCA-3′) and MCP-F/MCP-R (MCP-F, 5′-GACTTGGCCA CTTATGAC-3′; MCP-R, 5′-GTCTCTGGAGAAGAAGAA- 3′), were used to detect the transcripts of the known DE gene, dUTPase gene (*DUT*) [17], and L gene, major capsid protein gene (*MCP*) [18], respectively.

Subcellular localization assay. EPC cells were transfected with pEGFP-HSD or empty vector 3 using Lipofectamine reagent (Invitrogen). At 48 h after transfection, the cells were rinsed with PBS (pH 7.4) and fixed with 4% paraformaldehyde for 15 min. The cells were then rinsed with PBS and permeabilized with 0.2% Triton X-100 for 15 min. Afterwards, Hoechst 33258 (Sigma) was added at a final concentration of 1 μg/ml to stain the nucleus for 15 min. Finally, the cells were rinsed with PBS, mounted with 50% glycerol, and visualized under fluorescence microscope (Leica, Germany). To further evaluate the subcellular localization of RGV 3β-HSD in EPC cells, two organelle-specific markers, pDsRed2-ER and pDsRed2-Mito (Clontech), were used. The cotransfected EPC cells were observed by using confocal laser scanning microscope (Leica, Germany).

DNA transfection and selection of stable transfectants. EPC cells were transfected with pcDNA3.1-HSD or empty vector pcDNA3.1 using the above-mentioned method. Following transfection for 48 h, G418 (Amresco) was added to the medium at a final concentration of 400 μg/ml. After 4 weeks' selective culture, the transfected cells were confirmed by RT-PCR detection for the expression of RGV 3β-HSD gene. The stably pcNDA3.1 and pcDNA3.1-HSD-transfected EPC cells were termed EPC/pcDNA3.1 and EPC/pcDNA3.1-HSD.

Cell proliferation and viral replication kinetics assays. For cell proliferation assay, EPC/pcDNA3.1-HSD or EPC/pcDNA3.1 cells were seeded in 24-well plates at an initial concentration of 3×10^4 cells per well. The cell numbers from duplicate wells were counted by using haemacytometer under a light microscope daily until day 8. For viral replication kinetics assay, both the stably transfected EPC cells were grown in 24-well plates. RGV was then inoculated to the monolayer cells at an MOI of 5. After 1 h absorption, unbound virus was removed and then the cells were incubated in TC199 medium containing 5% FBS. At 0, 2, 8, 12, 16, 24, 36, and 48 h p.i., the cell cultures were harvested, freeze-thawed three times, and then titrated on duplicate monolayers of EPC cells. The morphological changes were observed under light microscope (Leica, Germany).

MTT assay. EPC/pcDNA3.1-HSD or EPC/pcDNA3.1 cells were seeded in 96-well plates at a concentration of 4×10^4 cells per well. RGV were inoculated to the cells at an MOI of 5. The mock-infected cells and the blank wells containing medium only were utilized as control. At indicated time p.i., the medium in each well was replaced by 100 μl fresh medium containing 0.5 mg/ml MTT. The plates were incubated in darkness at 25 °C for 4 h. The medium was then removed and the crystal formazan formed in each well was dissolved with 200 μl of dissolving solution containing 175 μl of dimethyl sulfoxide and 25 μl of glycine buffer (0.1 M glycine, 0.1 M NaCl [pH 10.5]). Absorbance was read at 570 nm using a microplate reader (Tecan Sunrise, Switzerland).

Results

Identification and sequence analysis of RGV 3β-HSD gene

Using the designed primers, an 1184 bp fragment was amplified from RGV. Sequence analysis revealed that the obtained fragment contained a complete ORF of RGV 3β-HSD gene (GenBank Accession No. DQ887345), which has 1068 bp in length, encoding a 355 aa predicted protein. The deduced amino acid sequence showed 46%, 45%, 45%, and 47% identity to human, bovine, mouse, and frog 3β-HSD, respectively. The highest identity to frog 3β-HSD suggests that the RGV 3β-HSD gene might be horizontally transferred from its natural host frog. An alignment of amino acid sequence of RGV 3β-HSD with human, bovine,

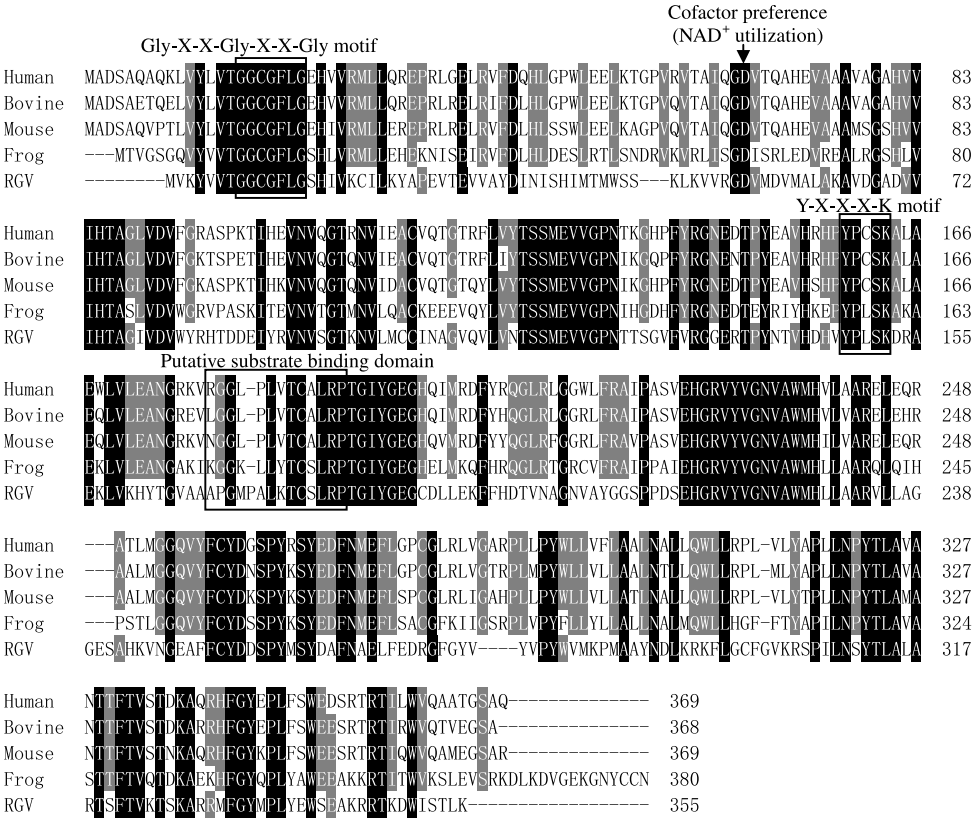

Fig. 1. Amino acid alignment of RGV 3β-HSD (ABI36881) with other 3β-HSDs from human (AAH04929), bovine (NP_001029868), mouse (AAG37823), and frog (AAH70664). Sequences with four identities in one position are highlighted in grey or black boxes. Four conserved domains of 3β-HSD are indicated according to the reference [8].

mouse, and frog 3β-HSD is shown in Fig. 1, and overall the proteins showed striking similarity. Upon the alignment, it was also revealed that RGV 3β-HSD contained the conserved amino acid residues that might represent some essential domains of 3β-HSD, such as Gly-X-X-Gly-X-X-Gly motif, confactor preference site, Y-X-X-X-K motif, and putative substrate binding domain (Fig. 1) [8].

RGV 3β-HSD gene is transcribed immediate-early from 19 nucleotides upstream of the translation start site during infection

The transcription initiation site of RGV 3β-HSD gene was determined by 5′-RACE. As a consequence, it was revealed that the major transcription initiation site of RGV 3β-HSD gene was located at 19 nucleotides upstream of the translation start site (Fig. 2A).

To analyze the temporal transcription of RGV 3β-HSD gene during infection *in vitro*, RT-PCR was performed to detect the transcript in RGV-infected EPC cells at different infection stages. The 345 bp 3β-HSD gene-specific fragment was detected at 4 h p.i. and continued high transcription until 48 h p.i. (Fig. 2B, upper panel). For internal control, the transcripts of cellular *β-actin* were consistent with each other (Fig. 2B, lower panel). For negative control, no 3β-HSD gene-specific PCR product was detected (data not shown), indicating that the extracted total RNA had no contamination of the viral genomic DNA.

To further classify the transcript of RGV 3β-HSD gene, the CHX and AraC inhibition assay was performed. The DE gene *DUT* [17] and L gene *MCP* [18] were chosen for control. As expected, the *DUT* transcript was detected in the AraC-treated sample infected with RGV for 48 h, and not in the CHX-treated sample infected with RGV for 6 h, whereas the transcription of *MCP* was inhibited in the presence of CHX and AraC, and was only presented in the sample infected with RGV at 48 h p.i. (Fig. 2C). In contrast, the transcript of 3β-HSD gene could be detected in all RGV-infected EPC cells regardless of the absence or presence of CHX and AraC (Fig. 2C), thus suggesting that RGV 3β-HSD gene is an IE viral gene.

RGV 3β-HSD is associated with the mitochondria in EPC cells

To assess the subcellular localization of RGV 3β-HSD, a recombinant plasmid pEGFP-HSD, which could express RGV 3β-HSD with a C-terminal EGFP tag, was constructed and transfected into EPC cells. Observation under fluorescence microscope showed that the strong green fluorescence was aggregated in cytoplasm near the nucleus in pEGFP-HSD transfected EPC cells (Fig. 3A, lower

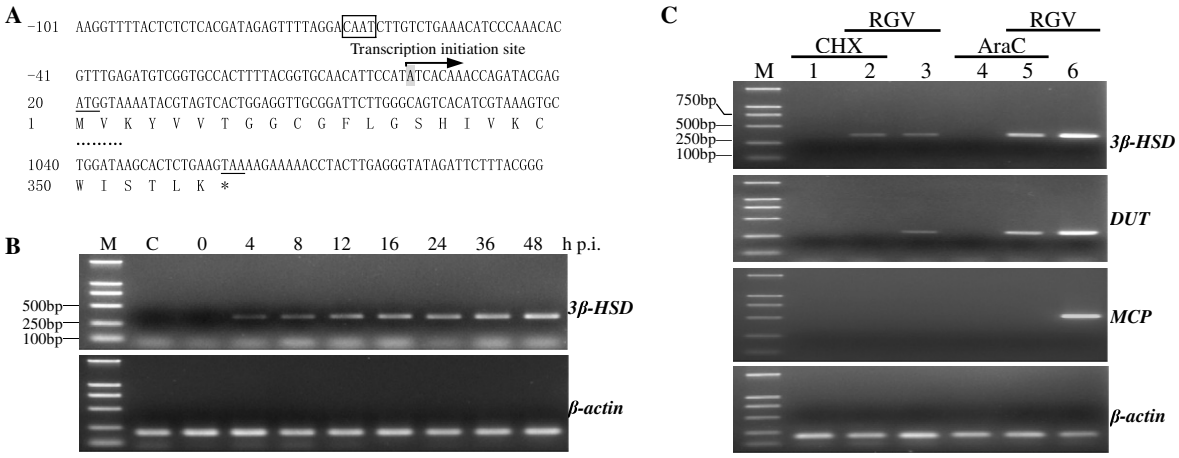

Fig. 2. Transcription analyses of RGV 3β-HSD gene. (A) Transcription initiation site of RGV 3β-HSD gene determined by 5′-RACE. A putative CAAT box in 5′ non-coding region is indicated. (B) Temporal transcription analysis of RGV 3β-HSD gene by RT-PCR. Total RNA was isolated from mock-infected (lane C) and RGV-infected EPC cells at different times p.i.; lane M, DL2000 DNA marker. (C) RT-PCR detection of RGV 3β-HSD gene transcripts under drug treatments. Total RNA was isolated from CHX-treated and/or RGV-infected EPC cells at 6 h p.i. (lanes 1–3), and from AraC-treated and/or RGV-infected EPC cells at 48 h p.i. (lanes 4–6).

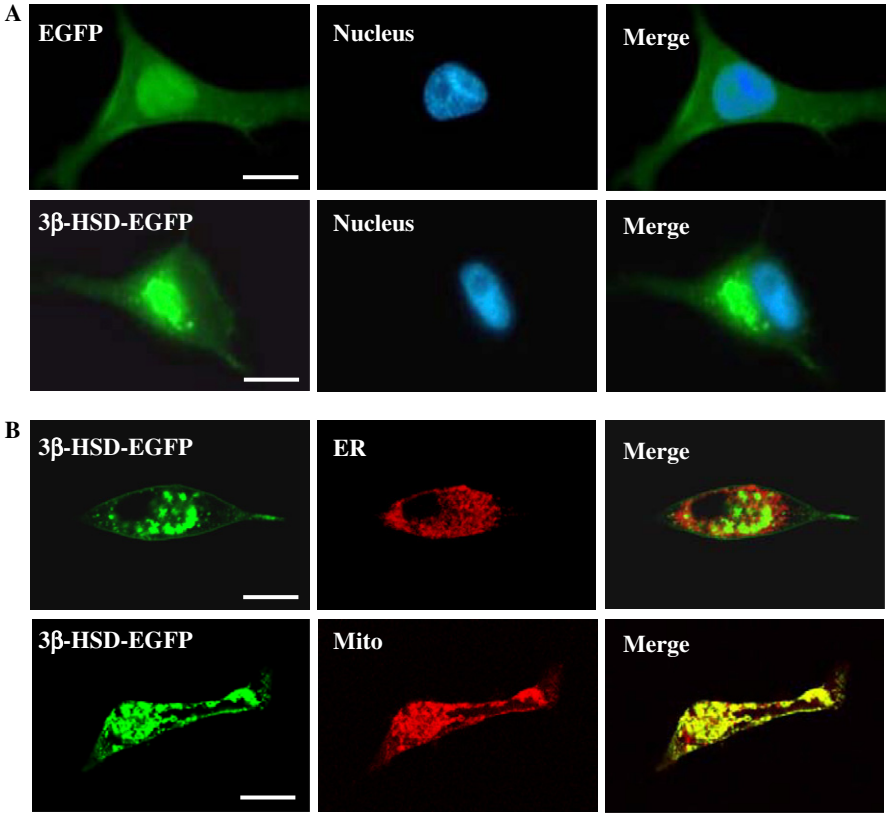

Fig. 3. Intracellular localization of RGV 3β-HSD. (A) Intracellular localization of RGV 3β-HSD by fluorescence microscopy. EPC cells were transfected with empty vector pEGFP-N3 (upper row) or pEGFP-HSD (lower row). The blue images show the localization of nucleus stained by Hoechst 33258. (B) Subcellular localization of RGV 3β-HSD by confocal microcopy. EPC cells were cotransfected with pEGFP-HSD+pDsRed2-ER (upper row) or pEGFP-HSD+pDsRed2-Mito (lower row). Red images show the localization of endoplasmic reticulum (ER) or mitochondria (Mito). Scale bar, 10 μm. (For interpretation of the references to color in this figure legend, the reader is referred to the web version of this paper.)

row), indicating that 3β-HSD-EGFP fusion protein was localized in the cytoplasm of EPC cells. As control, the vector-expressed EGFP was distributed in both the cytoplasm and the nucleus of EPC cells (Fig. 3A, upper row).

To further evaluate the precise localization of 3β-HSD-EGFP in the cytoplasm of EPC cells, two organelle-specific markers, pDsRed2-ER (specific for ER) and pDsRed2-Mito (specific for mitochondria), were used. Confocal

microscopy revealed that 3β-HSD-EGFP was exclusively colocalized with the mitochondria marker (pDsRed2-Mito) (Fig. 3B, lower row), whereas it showed no colocalization with the ER marker (pDsRed2-ER) (Fig. 3B, upper row), suggesting that RGV 3β-HSD is associated with the mitochondria in EPC cells.

No effect of RGV 3β-HSD overexpression on the growth of EPC cells and RGV replication

To study the effect of RGV 3β-HSD overexpression on the growth of host EPC cells and the replication of RGV, we cloned RGV 3β-HSD gene into a eukaryotic expression vector pcDNA3.1, which is under the control of a cytomegalovirus immediate-early gene promoter. The construct was transfected into EPC cells, and the stably transfected cells were screened with G418 and confirmed by RT-PCR detection (Fig. 4A). As shown in Fig. 4B, the growth curves of both stably transfected EPC cells showed that RGV 3β-HSD overexpression did not alter the proliferation characteristics of the host cells. Both kinds of stably transfected EPC cells displayed typical growth curves in a time-dependent way. On the other hand, to assess the effect of 3β-HSD overexpression on RGV replication, a one-step growth assay was performed. As shown in Fig. 4C, the one-step growth curves of RGV in both stably transfected EPC cells are very similar, while the virus titers yielded in 3β-HSD-expressing EPC cells were slightly higher (<1.5-fold) than that yielded in the vector-expressing cells from 12 to 48 h p.i.

Overexpression of RGV 3β-HSD suppresses RGV-induced cytopathic effect

Unexpectedly, apparent differences in morphology were observed in the both kinds of stably transfected EPC cells infected by RGV (Fig. 4D). At 12 h p.i., the CPE in vector-expressing EPC cells began to appear more serious with perceptible plaque than that in 3β-HSD-expressing EPC cells. The difference continued existence at 24, 36, and 48 h p.i., whereas at 72 h p.i., the CPE in both transfected cells seemed similar again: all cells were detached from the substratum and clumped together (data not shown), implying that the infected cells might have lost their most viabilities.

To corroborate the observation and to quantitatively determine the CPE, MTT assay was performed. As shown in Fig. 4E, fewer EPC/pcDNA3.1-HSD cells lost their viabilities after infection compared to the control cells of EPC/pcDNA3.1, which is quite consistent with the

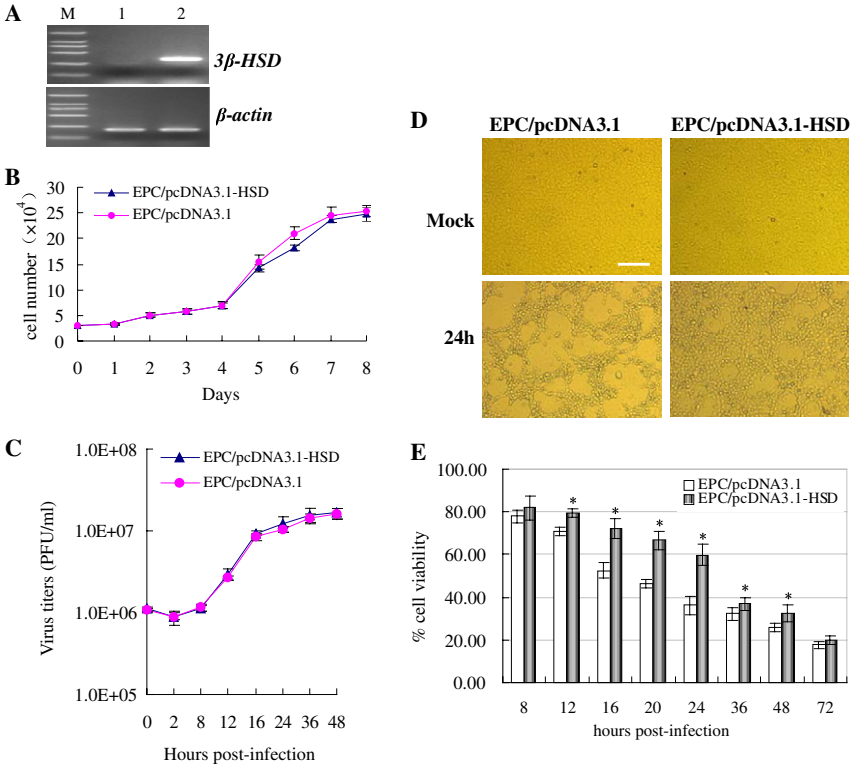

Fig. 4. Suppression of RGV-induced CPE by RGV 3β-HSD overexpression. (A) Confirmation of the stably transfected EPC cells by RT-PCR. lane M, DL2000 DNA marker; lane 1, EPC/pcDNA3.1; lane 2, EPC/pcDNA3.1-HSD. (B) Effect of 3β-HSD overexpression on the growth of host cells. Cell numbers were counted daily until day 8. (C) Effect of 3β-HSD overexpression on RGV replication. The virus titers were determined by plaque assay. (D) Morphological observation of RGV-induced CPE under light microscope. Scale bar, 200 μm. (E) Quantitative detection of RGV-induced CPE by MTT assay. The data are expressed as means ± standard deviation. Statistical analysis was performed by using the Student's *t*-test. Column bars with asterisks are significantly different with the corresponding controls at $p < 0.05$.

morphological observation. Statistically, there existed significant differences ($p < 0.05$) from 12 to 48 h p.i. between the means of cell viability percentage of the 3β-HSD-expressing and vector-expressing EPC cells infected with RGV, and the difference reached its highest level at 24 h p.i. with $59.9 \pm 4.8\%$ versus $36.1 \pm 4.4\%$. Therefore, both the morphological observation and MTT assay provide direct evidence that overexpression of RGV 3β-HSD in EPC cells could suppress or delay RGV-induced CPE.

Discussion

The structural features of early viral messages have been clarified in the studies of FV3, and the 5′ non-coding regions were generally found to be short, unstructured, and AU-rich [19]. RGV 3β-HSD gene 5′ non-coding region has only 19 nucleotides and contains 58% AU content, which are consistent with the features. Interestingly, compared with the promoter sequence of the IE gene encoding ICR489 [20], a consensus fragment of CAATCTTGT, including a putative CAAT box, was found to localize at bases −68 to −60 from the major transcription start site of RGV 3β-HSD gene (Fig. 2A). Further studies are needed to identify whether this consensus fragment in promoter region has a function of transcription regulation. Moreover, through the CHX and AraC inhibition assay, we revealed that RGV 3β-HSD gene is an IE viral gene, which could just verify its structural feature of 5′ non-coding region, and is also similar to the studies in the vaccinia virus 3β-HSD [10]. The immediate-early temporal expression of RGV 3β-HSD gene is consistent with a function either in transcription regulation or in host-virus interaction [6,7].

The subcellular localization of v3β-HSD has not been found in previous report. In this study, we revealed that RGV 3β-HSD is a mitochondria-localized protein in EPC cells by confocal microscopy. In addition, to avoid the bias of EPC cells, we also observed the same localization of 3β-HSD-EGFP in other fish cell line, fathead minnow (FHM) (data not shown). This mitochondrial localization of RGV 3β-HSD is different from the vertebrate 3β-HSDs, which have unique dual subcellular localization with ER and mitochondria [8]. The cellular organelle mitochondria are associated with many metabolic and biochemical processes including ATP production, intracellular calcium regulation, and apoptosis [21]. Large clusters of mitochondria were observed to distribute around the virus assembly sites during RGV infection [22]. Consequently, the mitochondrial localization of RGV 3β-HSD indicates that it might be a protein involved in host-virus interaction.

Furthermore, we proved that RGV 3β-HSD overexpression could suppress RGV-induced CPE. Additionally, we also observed that RGV 3β-HSD overexpression could inhibit the CPE induced by *Scophthalmus maximus* rhabdovirus (SMRV) (data not shown) [23]. This novel role of RGV 3β-HSD in inhibiting virus-induced CPE indicates that it should be a protein involved in host-virus interaction. The hypothesis is also consistent with the studies of the vaccinia virus 3β-HSD, which contribute to virulence by inhibiting inflammatory response to infection [9,10]. But what does the virus benefit from the suppression of CPE? One possible explanation may be that the CPE was suppressed or delayed by 3β-HSD during infection so that the virus could have enough time to replicate and yield progeny virus. However, the yield of RGV in EPC/pcDNA3.1-HSD cells only showed a slight increase compared with that in the vector-expressing EPC cells (Fig. 4C). It might be caused by the effect that RGV itself could also express 3β-HSD during infection, as the 3β-HSD gene-deleted vaccinia virus showed 2- to 3-fold reduction in yield of virus compared with wild type virus during single step growth [10].

In conclusion, we have identified a 3β-HSD gene from RGV. It is transcribed immediate-early and encodes a mitochondria-localized protein. Furthermore, overexpression of RGV 3β-HSD could suppress virus-induced CPE. From discussed above, all evidence suggest that RGV 3β-HSD might be a protein involved in host-virus interaction.

Acknowledgment

This study was supported by grants from the National Major Basic Research Program (2004CB117403), the National Natural Science Foundation of China (30671616).

References

[1] Q.Y. Zhang, Z.Q. Li, Y.L. Jiang, S.C. Liang, J.F. Gui, Preliminary studies on virus isolation and cell infection from disease frog *Rana grylio*, Acta Hydrobiol. Sin. 20 (1996) 390–392 (Chinese with English abstract).

[2] Q.Y. Zhang, Z.Q. Li, J.F. Gui, Studies on morphogenesis and cellular interactions of *Rana grylio* virus in an infected fish cell line, Aquaculture 175 (1999) 185–197.

[3] Q.Y. Zhang, F. Xiao, Z.Q. Li, J.F. Gui, J.H. Mao, V.G. Chinchar, Characterization of an iridovirus from the cultured pig frog (*Rana grylio*) with lethal syndrome, Dis. Aquat. Org. 48 (2001) 27–36.

[4] V.G. Chinchar, S. Essbauer, J.G. He, A. Hyatt, T. Miyazaki, V. Seligy, T. Williams, Iridoviridae, in: C.M. Fauquent, M.A. Mayo, J. Maniloff, Ul. Desselberger, L.A. Ball (Eds.), Virus Taxonomy: 8th Report of The International Committee on the Taxonomy of Viruses, Elsevier, London, 2005, pp. 163–175.

[5] T. Williams, V. Barbosa-Solomieu, V.G. Chinchar, A decade of advances in iridovirus research, Adv. Virus Res. 65 (2005) 173–248.

[6] D.B. Willis, R. Goorha, V.G. Chinchar, Macromolecluar synthesis in cells infected by frog virus 3, Curr. Top Microbiol. Immunol. 116 (1985) 77–106.

[7] B. Moss, J.L. Shisler, Immunology 101 at poxvirus U: immune evasion genes, Semin. Immunol. 13 (2001) 59–66.

[8] J. Simard, M.L. Recketts, S. Gingras, P. Soucy, F.A. Feltus, M.H. Melner, Molecular biology of the 3β-hydroxysteroid dehydrogenase/$\Delta^5 - \Delta^4$isomerase gene family, Endocr. Rev. 26 (2005) 525–582.

[9] P.C. Reading, J.B. Moore, G.L. Smith, Steroid hormone synthesis by vaccinia virus suppresses the inflammatory response to infection, J. Exp. Med. 197 (2003) 1269–1278.

[10] J.B. Moore, G.L. Smith, Steroid hormone synthesis by a vaccinia enzyme: a new type of virus virulence factor, EMBO J. 11 (1992) 1973–1980, [published erratum at 11, 3490].

[11] M.E. Baker, R. Blasco, Expansion of the mammalian 3β-hydroxysteroid dehydrogenase/plant dihydroflavonol reductase superfamily to include a bacterial cholesterol dehydrogenase, a bacterial UDP-galactose-4-epimerase, and open reading frames in vaccinia virus and fish lymphocystis disease virus, FEBS Lett. 301 (1992) 89–93.
[12] V. Sroller, L. Kutinova, S. Nemeckova, V. Simonova, V. Vonka, Effect of 3-β-hydroxysteroid dehydrogenase gene deletion on virulence and immunogenicity of different vaccinia viruses and their recombinants, Arch. Virol. 143 (1998) 1311–1320.
[13] J.G. He, L. Lv, M. Deng, H.H. He, S.P. Weng, X.H. Wang, S.Y. Zhou, Q.X. Long, X.Z. Wang, S.M. Chan, Sequence analysis of the complete genome of an iridovirus isolated from the tiger frog, Virology 292 (2002) 185–197.
[14] W.G.H. Tan, T.J. Barkman, V.G. Chinchar, K. Essani, Comparative genomic analyses of frog virus 3, type species of the genus *Ranavirus* (family *Iridoviridae*), Virology 323 (2004) 70–84.
[15] S.F. Altschul, T.L. Madden, A.A. Schäffer, J. Zhang, Z. Zhang, W. Miller, D.J. Lipman, Gapped BLAST and PSI-BLAST: a new generation of protein database search programs, Nucleic Acids Res. 25 (1997) 3389–3402.
[16] J.D. Thompson, T.J. Gibson, F. Plewniak, F. Jeanmougin, D.G. Higgins, The ClustalX windows interface: flexible strategies for multiple sequence alignment aided by quality analysis tools, Nucleic Acids Res. 24 (1997) 4876–4882.
[17] Z. Zhao, F. Ke, J.F. Gui, Q.Y. Zhang, Characterization of an early gene encoding for dUTPase in *Rana grylio* virus, Virus Res. (2006) doi:10.1016/j.virusres.2006.08.007.
[18] J. Mao, T.N. Tham, G.A. Gentry, A.M. Aubertin, V.G. Chinchar, Cloning, sequence analysis, and expression of the major capsid protein of the iridovirus frogvirus 3, Virology 216 (1996) 431–436.
[19] V.G. Chinchar, Ranaviruses (family *Iridoviridae*): emerging cold-blooded killers, Arch. Virol. 147 (2002) 447–470.
[20] W. Beckman, T.N. Tham, A.M. Aubertin, D.B. Willis, Structure and regulation of the immediate-early frog virus 3 gene that encodes ICR489, J. Virol. 62 (1988) 1271–1277.
[21] P. Boya, A.L. Pauleau, D. Poncet, R.A. Gonzalez-Polo, N. Zamzami, G. Kroemer, Viral proteins targeting mitochondria: controlling cell death, Biochim. Biophys. Acta 1659 (2004) 178–189.
[22] X.H. Huang, Y.H. Huang, X.P. Yuan, Q.Y. Zhang, Electron microscopic examination of the viromatrix of *Rana grylio*virus in a fish cell line, J. Virol. Meth. 133 (2006) 117–123.
[23] C. Du, Q. Zhang, C. Li, D. Miao, J. Gui, Induction of apoptosis in a carp leucocyte cell line infected with turbot (*Scophthalmus maximus*) L. rhabdovirus, Virus Res. 101 (2004) 119–126.